

On the influence of metastable states and the behavior of the EEDF in the characterization of the negative glow of a N₂-Ar discharge by OES

Isola L.¹, López M.¹, Gómez B. J.¹ and Guerra V.²

¹Instituto de Física Rosario (CONICET-UNR) 27 Febrero 210 Bis. (2000) Rosario, Argentina.

²Instituto de Plasmas e Fusão Nuclear, Instituto Superior Técnico, 1049-001 Lisboa, Portugal

E-mail: isola@ifir-conicet.gov.ar

Abstract.

Optical emission spectroscopy (OES) is an essential diagnostic technique in many plasma systems, such as those used for surface treatments or fabrication of thin films. Despite the simplicity of application of OES, its interpretation is not straightforward. In particular, it requires the use of models, which due to the complexity and variety of discharge conditions, have not yet been fully understood [1]–[3].

In addition, Langmuir probes have been widely used to characterize plasmas. They allow the measurement of several parameters of interest, such as the electron density and temperature, as well as the determination of the electron energy distribution function (EEDF) by numerical derivation of the characteristic $V - I$ [4] or by probe-current modulation [5].

In this work, some second positive system bands in the negative glow of an Ar-N₂ plasma at a pressure of 2.5 Torr were investigated both by OES and Langmuir probes, for different mixture concentrations. The main purpose of this study was to verify how metastable states and the behavior of the EEDF may influence the interpretation of OES data.

1. Introduction

Optical emission spectroscopy (OES) methods based on spectral band head ratios have been used to determine electron properties of N₂ plasmas, such as electron temperature and density [1, 2, 6]. However, these methods cannot be directly applied to Ar – N₂ gas mixtures because of the high excitation transfer of N₂ from Ar(³P_{2,0}) metastable atoms [6]. In fact, this process produces a characteristic vibrational and rotational distribution in the *second positive system* (SPS) [7, 8], with an overpopulation of high rotational levels ($K > 30$), producing an overlap between the vibrational bands belonging to the same vibrational family. Hence it is not possible to identify the contribution of each vibrational band in the measured spectrum.

Therefore, the simulation of the bands, taking into account the possible excitation processes, becomes essential.

On the other hand, the methods based on the band head ratio use a Maxwellian EEDF, but this assumption is often inaccurate.

In this work, we studied the discharge kinetics, through the analysis and fitting of the band structure at 380.49 nm (N₂(C³Π_u⁺, v' = 0 → B³Π_g⁺, v'' = 2)) and 375.54 nm (N₂(C³Π_u⁺, v' = 1 → B³Π_g⁺, v'' = 3)), belonging to the SPS, and the EEDF behavior with the variation of the Ar concentration in the gas mixture.

2. Experimental set-up

The plasma reactor used consists of a stainless steel chamber of 254 mm in diameter and 360 mm in height, with two side glass windows (Figure 1). The work pressure and the gas flow rate were



kept constant at 2.5 Torr and 100 ml/min respectively. The discharge was generated between a central disc, which works as a cathode, and the walls of the chamber. A variable pulsed source with a frequency of 100 Hz and duty cycle of 0.7 was used, keeping the voltage constant at -500 V.

The optical emission spectra from the discharge were recorded with a Jarrell-Ash monochromator with Czerny-Turner mounting. The slit entry was set at $25 \mu\text{m}$, whereas the grating used was 3600 grooves/mm. A lens focused the light to the monochromator, and a linear arrangement of 1024 photodiodes was used as detector.

Concerning the probe measurements, a cylindrical Langmuir probe consisting of a tungsten wire of radius $R = 15 \mu\text{m}$ and $L = 60$ mm in length was employed. It was fed by a variable (from 0 to -40 V) source. A small AC sine voltage with frequency 1 KHz was superimposed on the DC probe bias, then the second derivative of the probe characteristic was obtained directly from measuring the current component with frequency 2 KHz [9]. This measurement was performed with a Lock-in amplifier. It is worth mentioning that the measurements were performed in a DC plasma due to the impossibility of measuring with the Lock-in in a pulsed plasma.

The electron energy distribution function $g(\varepsilon)$ can then be obtained from the second derivative of the probe characteristic curve,

$$g_e(\varepsilon) = \frac{2m}{e^2 A} \left(\frac{2\varepsilon V}{m} \right)^{\frac{1}{2}} \frac{d^2 I_e}{dV^2} \quad (1)$$

where ε denotes the electron energy, m the electron mass, V is the probe voltage with respect to the plasma potential, A is the area of the probe, and the maximum of the first derivative has been taken as the plasma potential.

Both the optical emission spectroscopy and the Langmuir probe measurements were made at the same position in the discharge chamber, marked in Figure 1 by h , being $h = 10.25$ mm.

3. Measurements

3.1. Spectroscopy

In this work, bands of the SPS were studied by spectroscopy for different mixture concentrations. Typical spectra are shown in Figure 2.

3.2. Fitted Bands

The bands were fitted using the least squares method. The band intensities $v' = 0 \rightarrow v'' = 2$ and $v' = 1 \rightarrow v'' = 3$ of the SPS $N_2(C^3\Pi_u) \rightarrow N_2(B^3\Pi_g)$ (with band heads in 380.49 nm and 375.54 nm) are given by :

$$I_{CB}(\lambda, T_{\text{rot}}, N_o, \delta\lambda, \Delta\lambda, X) = N_o(\lambda, v', T_{\text{rot}}) A_{CB}(v', v'') \sum_{i=P,R,Q} \sum_{\Omega=0,1,2} \sum_{J'} \exp\left(\frac{-BhcJ'(J'+1)}{k_B T_{\text{rot}}}\right) \exp\left(\frac{-4\ln(2) [\lambda + \Delta\lambda - \lambda_{\Omega}^i(J')]^2}{(\delta\lambda)}\right) S_{\Omega}^i(J') X(J') \quad (2)$$

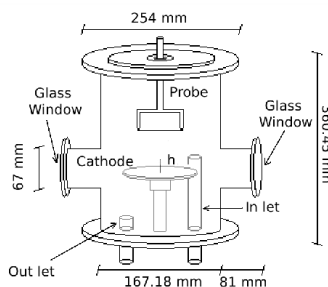


Figure 1. Experimental set-up

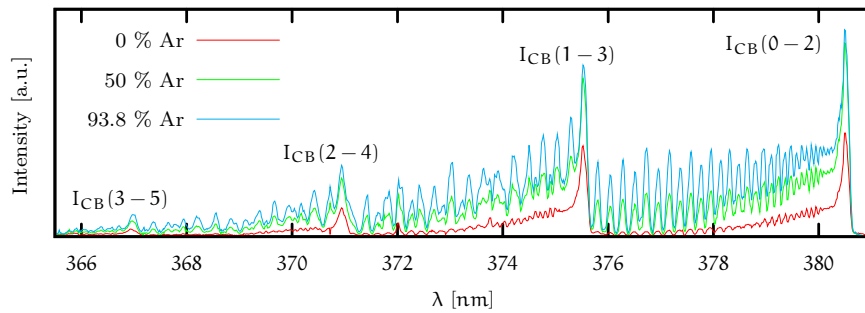


Figure 2. Vibrational bands with $\Delta v = v' - v'' = -2$ belonging to the SPS, for different Ar concentrations.

where N_o includes the spectral response, the density in the upper level and partition function, $\delta\lambda$ the full width at half maximum of the rotational line, $\Delta\lambda$ a small shift in the wavelength, $A_{CB}(v', v'')$ is the Einstein coefficient [10], B the rotational constant, $S_Q^i(J'_i)$ is the Hönl-London factor [11] and $X(J')$ is a fitting parameter that allows the alternation between K even and odd that occurs because of the collision with $Ar(^3P_2)$, when we increase the Ar concentration (see Figure 3). Finally, in the bands area of 375.54 nm and 380.49 nm there are some lines of Ar

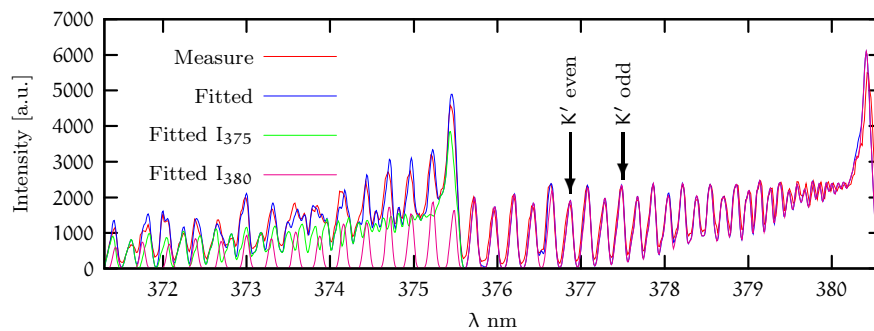


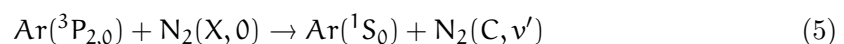
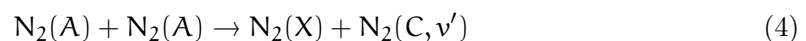
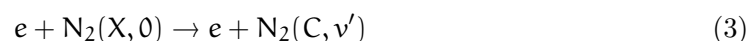
Figure 3. Overlapping bands 380.49 nm and 375.54 nm in a discharge with high Ar concentration (93.75% Ar). Measured and fitted bands.

and Fe, which were taken into account to fit these bands, using the line intensities as fitting parameters.

3.3. Kinetic model

To analyze these spectra we used a simple model for the negative glow kinetics, described by the following assumptions:

- (i) The main excitation reactions of state $N_2(C, v')$ are



- (ii) Levels $N_2(C, v')$ and $N_2^+(B, v')$ are primary lost by radiative decay.

3.4. Model Discussion

3.4.1. Excitation by e When $N_2(C^3\Pi_u)$ is populated by electron impact from the ground state, the vibration distribution can be approximated by the Franck-Condon coefficient [10]. The rotational distribution is taken to be unchanged in the excitation by electron impact, then the $N_2(C^3\Pi_u)$ rotational distribution will correspond to the $N_2(X^1\Sigma_g^+)$ rotational distribution. Note that the rotational population is distributed between the P, Q and R branches, belonging to $C^3\Pi_u$ level, following the Hönl-London factor [11].

3.4.2. Excitation by $N_2(A)$ The pooling reaction (4) produces an overpopulation of the level $N_2(C^3\Pi_u, v = 1)$ (see Table 1 [12]). This overpopulation in $v = 1$ is not observed in our N_2 discharge, giving an *a posteriori* confirmation that the pooling reaction does not contribute significantly to the production of the $N_2(C^3\Pi_u)$ state.

3.4.3. Metastable Ar The $Ar(^3P_0)$ is less efficient than $Ar(^3P_2)$ in excitation transfer to $N_2(C^3\Pi_u)$. In addition, its concentration is smaller, then all the excitation transfer is in fact produced by $Ar(^3P_2)$.

The collision (5) is an exothermic process (Table 2), then it produces excited molecules $N_2(C)$ with large rotational energies, particularly for $v' = 0$. This process also produces an intensity alternation between even and odd K' rotational levels, which is not expected in a Π state [13]. The population of different $N_2(C)$ vibrational states cannot be explained by the Franck-Condon factor and the rate coefficients shown in Table 1 (from $v = 0$) [14] should be used.

Table 1. Franck-Condon coefficients and rate coefficients [$10^{-11} \text{cm}^{-3} \text{s}^{-1}$]

	$q_{0v'}$	$k_{N_2(A,0)-N_2(A,0)}^{v'}$	$k_{Ar-N_2}^{v'}$
$N_2(C, 0)$	0.55	2.6 ± 0.1	2.9 ± 0.3
$N_2(C, 1)$	0.31	4.1 ± 0.2	0.60 ± 0.07
$\frac{N_2(C,1)}{N_2(C,0)}$	0.56	1.58	0.21

Table 2. Exothermic $\Delta E(^3P_j, v')$ (meV) for the excitation transfer process

Initial State	$v' = 0$	$v' = 1$	$v' = 2$	$v' = 3$
3P_0	701	444	205	-28
3P_2	526	269	30	-203

The addition of vibrational energy to $N_2(X)$ gives increased vibrational excitation in $N_2(C)$, up to at least $v' = 4$ [8].

4. Results

4.1. Spectroscopy

Figure 4 shows how the intensity of the bands at 380.49 nm and 375.54 nm increase with the Ar concentration. Notice that the raise in the intensity of the band at 375.54 nm is slower. This can be seen very clearly in Figure 5. It should be note that the band intensities were calculated from the area under the fitted bands.

To perform a preliminary analysis of the results, it can be assumed that most of the $N_2(X)$ molecules have a vibrational state $v = 0$. Thus, for a N_2 discharge the ratio between the $N_2(C, v' = 1)$ and $N_2(C, v' = 0)$ densities should be close to the Franck-Condon coefficient ratio, while for a high Ar concentration discharge, this ratio should be close to the relation between the rate coefficients $K_{N_2-Ar}^{v'}$.

Figure 5 shows how this ratio changes from 0.65 to 0.39, which agrees qualitatively with the ratio between Franck Condon factors (0.56) and the ratio between the rate coefficient (0.21). Obviously, this difference is obtained because there is a vibrational distribution in the ground state $N_2(X)$.

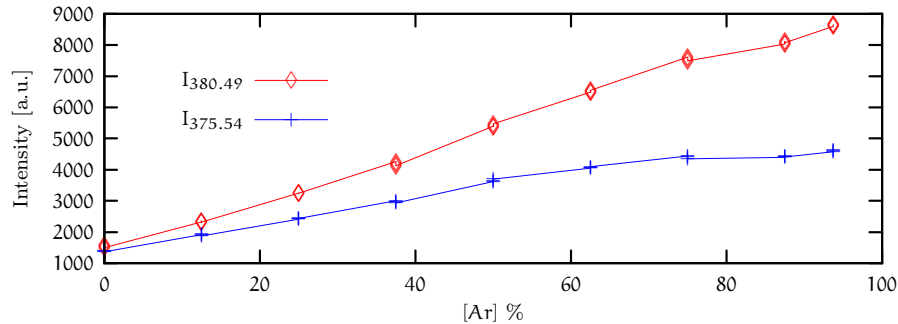


Figure 4. Emission intensity of bands 380.49 nm and 375.54 nm as a function of the Ar concentration

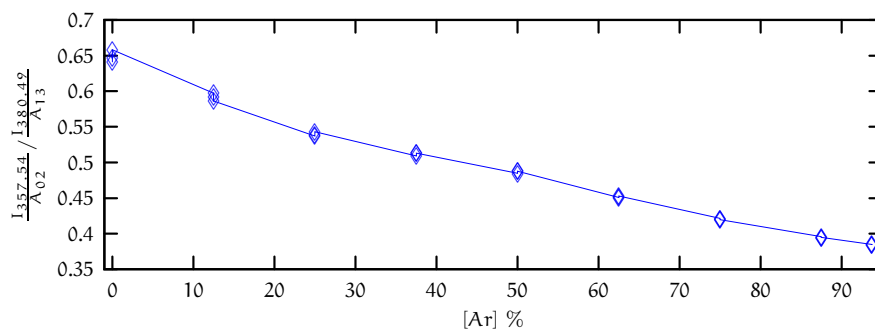


Figure 5. Ratio between $\frac{I_{375.54}}{A_{CB(1,3)}}$ and $\frac{I_{380.49}}{A_{CB(0,2)}}$ as a function of the Ar concentration

Another important result is observed with rotational temperatures of the SPS bands (Figure 6). Both bands have the same temperature (approximately 740 K) at 100% of N_2 , which agrees with the fact that the main mechanism of excitation is the collision with electrons from the ground state (reaction (3)), as proposed by the model. Then, when the Ar concentration is increased, the rotational temperatures reach 1960 K for 375.54 nm and 2510 K for 380.49 nm, in 93.75% of Ar where the main mechanism is the reaction (3). This higher temperature of 380.49 nm can be understood because the energy excess to excite the level $N_2(C, v' = 0)$ is greater than the energy excess to excite the level $N_2(C, v' = 1)$ (See Table 2).

4.2. Langmuir Probe

Figure 7 shows the EEDFs as a function of the Ar concentration. As can be seen, the electron density and electron temperature increase with the Ar content. Moreover, the EEDF deviates from a Maxwellian distribution in all cases. Work is in progress to include this effects in a model allowing the determination of the electron energy and temperature in $N_2 - Ar$ mixtures.

5. Conclusions

The rotational and vibrational structures of the SPS of N_2 are strongly influenced by the collisions between N_2 molecules and metastable Ar atoms. Therefore, any scheme designed to characterize the plasma by OES must take into account this excitation mechanism.

The relation between the populations of levels $N_2(C, v' = 1)$ and $N_2(C, v' = 0)$ gives information on the excitation mechanisms of $N_2(C)$. However, to perform quantitative analysis

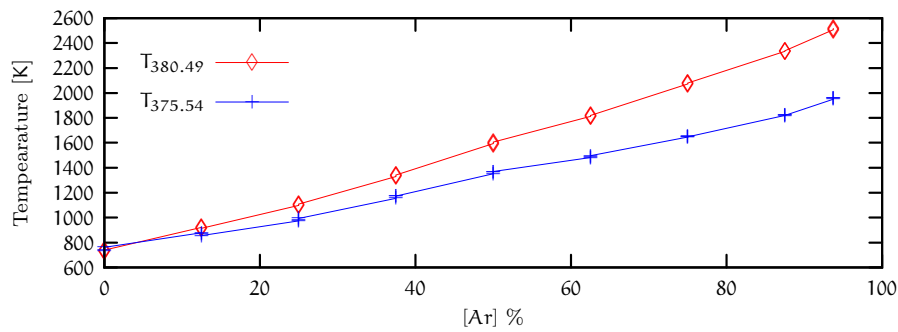


Figure 6. Rotational Temperature as a function of the Ar concentration

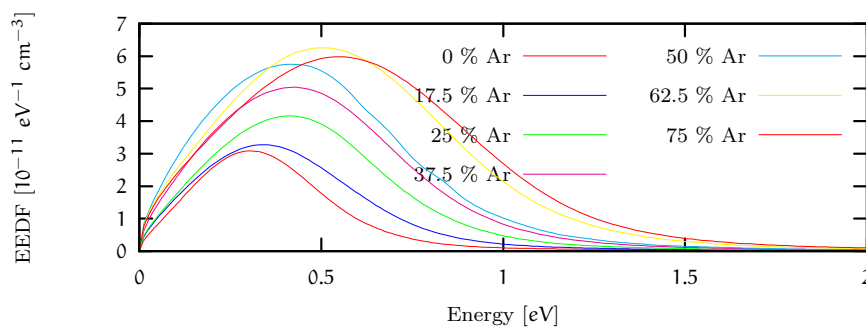


Figure 7. EEDF as a function of the Ar concentration

it is necessary to know the vibrational distribution function of $N_2(X)$, which is not easy to measure.

The electron density and temperature increases with the Ar content of the mixtures. Furthermore, the EEDFs differ quite significantly from Maxwellian distributions. This reveals the need of using EEDFs with an accurate information on the electron kinetics in the discharge in order to realistically characterize the plasma by OES.

Acknowledgments

The authors would like to thank Ing. Aldo Marenzana for this valuable collaboration in the development of the instrumentation. We award a grateful acknowledgment to Conicet (Argentina) and to the “Agencia Nacional de Promoción Científica y Tecnológica” (National Agency for Scientific and Technologic Promotion), Argentina, PICT 12-01981/2008-0374 and Josefina Prats Foundation.

References

- [1] Isola L M, Gómez B J and Guerra V 2010 *Journal of Physics D: Applied Physics* **43** 202
- [2] Zhu X and Pu Y 2008 *Plasma Sources Science and Technology* **17** 1–6
- [3] Debal F, Bretagne J, Jumet M, Wautelet M, Dauchot J P and Hecq M 1998 *Plasma Sources Science and Technology* **7** 219–229
- [4] Magnus F and Gudmundsson J T 2008 *Review of Scientific Instruments* **79**
- [5] Dietrich S, Christ-Koch S, Fantz U and Crowley B 2007 **28** ICPIG, July 15–20, 2007, Prague, Czech Republic
- [6] Britun N, Gaillard M, Ricard A, Kim Y M, Kim K S and Han J G 2007 *J. Phys. D: Appl. Phys.* **40** 1022–1029
- [7] Nguyen T D and Sadeghi N 1983 *Chemical Physics* **79** 41–55
- [8] Setser D W and Stedman D H 1970 *J. Chem. Phys.* **53** 1004–1020
- [9] Banner G R, Friar E M and Medicus G 1963 *The review of scientific instruments* **34** 231–237
- [10] Lofthus A and Krupenie P H 1977 *J. Chem. Phys. Ref. Data* **6** 113
- [11] Hartmann G and Johnson P C 1978 *J. Phys. B: Atom Molec. Phys.* **9** 1597–1612
- [12] Piper L G 1988 *J. Chem. Phys.* **216** 231–239
- [13] Derouard J, Nguyen T D and Sadeghi N 1980 *J. Chem. Phys.* **12** 6698–6705
- [14] Sadeghi N, Cheaib M and Setseters D W 1989 *J. Chem. Phys.* **90** 219–231